RSC Sustainability

ROYAL SOCIETY OF CHEMISTRY

PAPER

View Article Online
View Journal | View Issue

Cite this: *RSC Sustainability*, 2026, **4**, 952

Unprecedently high dissolution and depolymerization of hard-to-dissolve polyurethane in deep eutectic solvents under low-energy white light

Harmandeep Kaur,[a] Rajwinder Kaur,[a] Muskan,[a] Manpreet Singh,[a] Ravi Dutt,[a] Kanica Sharma,[a] Harjinder Singh,[a] Kuldeep Singh,[bc] Arvind Kumar,[bc] Gurbir Singh[d] and Tejwant Singh Kang *[a]

Polyurethane (PU), a synthetic polymer, is of immense commercial use. However, its utility and processing are limited by its negligible solubility in available solvents and by its non-biodegradable nature. Herein, a new sustainable approach for the unprecedentedly high dissolution (70 w/w%) and depolymerization of PU to a low-molecular-weight (900–3000 g mol^{-1}) depolymerized product is established. PU is dissolved in deep eutectic solvents (DESs) comprising lactic acid (LA) and $ZnCl_2$ under white light at 60 °C, and the dissolved material was regenerated using water. The multi-technique characterization of the regenerated material evidenced the cleavage of urethane linkages and the emergence of new functional groups. The impact of changes in the DES component ratio on its efficiency towards dissolution and depolymerization of PU highlighted the crucial role played by $ZnCl_2$. The DESs have been reused, and the properties of the regenerated material from recycled DES resemble those obtained from native DESs. This environmentally friendly approach simplifies PU processing and is expected to encourage the development of new metal-based DESs for handling a variety of non-biodegradable and hard-to-dissolve polymers. Further, reusability of DESs is expected to elevate the benefit-cost ratio to 15.723, making this process economically viable and attractive for industrial use.

Received 15th June 2025
Accepted 9th December 2025

DOI: 10.1039/d5su00436e

rsc.li/rscsus

Sustainability spotlight

This work addresses a problem involving environmental and technical challenges due to the persistence and poor recyclability of polyurethane. Understanding these issues is important for mitigating environmental harm and overcoming the limitations of existing recycling methods with the adoption of economically viable solutions like DESs for polymer processing and recycling. The sustainable advancement lies in the development of a green, energy-efficient, and economically viable process for dissolving and depolymerizing polyurethane using reusable, benign DESs, offering a scalable solution for described problem. This work advances SDG 12 (Responsible Consumption and Production), SDG 13 (Climate Action), and SDG 9 (Industry, Innovation, and Infrastructure), and supports SDG 14 and SDG 15, by reducing environmental plastic pollution through sustainable, green-chemistry solutions for polymer waste management.

Introduction

Plastics represent a diverse category of polymeric entities encompassing ubiquitous utilization.[1] Among these, polyurethane (PU) stands out as one of the favourite materials across a broad spectrum of end-user applications,[2–4] and the current annual production of PUs is estimated to be 20 million tons,[5,6] which is expected to increase further. However, PU's ineffective biodegradation, non-sustainable methods of processing with relatively lower yields, and inappropriate waste management infrastructure result in substantial volumes of PU waste leaking into the ecosystem.[7] Such leakage with long-term survival in the environment,[8,9] along with PU's resistance to heat, light, and toxins, is a major obstacle for its sustainable utilization. The inherent structural aspects of PU comprising hard segments (isocyanates such as 2,4 (or 2,6)-toluene diisocyanate (TDI) and 4,4′-diphenylmethane diisocyanate (MDI)), soft segments (polyester polyols or polyether polyols or glycols and other functional groups *etc.*),[8] central to which is the "urethane linkage", make this polymer hard to process in a sustainable manner. The conjunction of the urethane bond with extensive H-bonding in the polymer further hinders the dissolution, depolymerization and processing of PU in

[a]*Department of Chemistry, UGC-Centre for Advance Studies – II, Guru Nanak Dev University, Amritsar, 143005, India. E-mail: tejwantsinghkang@gmail.com*
[b]*Academy of Scientific and Industrial Research (ACSIR), Ghaziabad, 201002, India*
[c]*CSIR-Central Salt and Marine Chemicals Research Institute (CSIR), G. B. Marg, Bhavnagar, 364002, Gujarat, India*
[d]*Department of Chemistry, Khalsa College, Amritsar, 143002, India*

conventional solvents under optimal conditions of temperature and pressure.

In the past, several methods have been explored for the dissolution and processing of PU, including chemical hydrolysis,[10] biological degradation,[11] thermal degradation,[12] photochemical degradation,[13] organo-catalytic degradation and mechanical methods.[14] The chemical hydrolysis of PU materials requires acidic or alkaline conditions at relatively high temperatures (150–300 °C).[14–16] Similarly, thermal degradation also requires very high temperatures.[17,18] In organo-catalytic degradation, PU is pre-treated with solvents such as decalin or 1-methylnapthalene and tetralin before pyrolysis. The involvement of toxic solvents, high cost, formation of side products, and instability of the organo-catalyst are some of the disadvantages of this process.[19] Mechanical processes are quite tedious and result in low-grade plastic materials.[20,21] Enzymes, microorganisms, or a combination of both have been investigated for their ability to degrade PU; however, the slow degradation rate limits the practical applicability.[9,11] It is clear that these methods have various limitations, which, together with the high expense and energy usage, have prompted the scientific community to scrutinize green chemistry goals towards the degradation of plastic materials.

One such method is the dissolution, processing and regeneration of hard-to-dissolve materials in relatively greener solvents, such as ionic liquids (ILs)[22–24] and deep eutectic solvents (DESs).[25,26] DESs represent a new class of sustainable and green solvents, formed by mixing H-bond donors (HBD) and H-bond acceptors (HBA) in an appropriate ratio,[27,28] and have many remarkable properties akin to ILs.[29] Along with this, DESs have some additional advantages, such as ease of synthesis, low cost, and the use of non-toxic and biodegradable components for their synthesis,[27–30] which proclaim them to be green solvents. In the recent past, metal-based DESs have emerged as potential entities for the dissolution of hard-to-dissolve biopolymers (lignin,[31,32] chitin,[33] cork,[34] keratin[35]) and synthetic polymers, such as polythene (PE),[36] polyethylene terephthalate (PET),[37,38] poly(ethylene 2,5-furandicarboxylic acid) (PEF),[39] and polycarbonate.[40]

Following this, Deng *et al.* reported the dissolution (0.4 g of PU in 4 g of DES, solubility ~10 w/w%) and degradation of PU *via* the solvothermal method in an autoclave (140–180 °C for 6–8 h) in choline chloride (ChCl) and urea-based DES.[41] It was observed that the carbamate and urea links in the PU were cleaved while preserving the carbonate bond, which resulted in the formation of polycarbonate diol (PCDL) and 3,3-dimethyl-[1,1-biphenyl]-4,4-diamine (*o*-toluidine). Recently, Nataraj *et al.* also reported the degradation of PU by solvothermal process in an autoclave (180–200 °C for 12 h) employing ChCl and ferric chloride-based DESs in the presence of water and observed the formation of carbonaceous material with a yield of ~3%.[42] These reports have demonstrated the utility of DESs for converting PU into value-added materials, but the methods are limited by the use of high temperature and pressure conditions while displaying a low dissolution yield. Therefore, new DESs should be tested for the high solubilization and depolymerization of PU under sustainable conditions at relatively low temperatures and at atmospheric pressure. In this methodology, the conjunction of metal-based recyclable DES with white light has furthered the sustainability.

Scheme 1 Pictorial presentation of dissolution of PU in DES (LA : $ZnCl_2$ = 1 : 1) and its regeneration using water.

Herein, a new and sustainable strategy for the dissolution (solubility ~70 w/w%) and depolymerization of PU in $ZnCl_2$ and lactic acid (LA)-based DESs under white light at 60 °C is reported. The dissolved PU has been successfully regenerated using water as an antisolvent at room temperature (Scheme 1), and the regenerated material was characterized for possible degradation and transformation in molecular structure employing various state-of-the-art techniques. The regenerated low-molecular-weight material exhibits signatures of different functional groups, such as ester, alcohol, amine and amide, devoid of urethane linkages. The relative molar ratio of $ZnCl_2$ and LA was found to affect the extent of dissolution and depolymerization. The recovered DESs have been reused successfully for the dissolution and degradation of PU again, which establishes the sustainable nature of the process. It is expected that such a high solubility of PU, along with its depolymerisation, would establish a new platform for the processing and functionalization of a variety of hard-to-dissolve polymers to achieve sustainable development goals.

Results and discussion

For better understanding, the dissolution process of polyurethane (PU) in LA : $ZnCl_2$ (1 : 1) is discussed first, if not mentioned otherwise. PU does not solubilize in the given DES at room temperature under white light. At 60 °C under white light, PU tends to solubilize, achieving the highest solubility reported ever, *i.e.*, ~70 w/w% in 24 h. The transformation of a clear yellowish DES to a blackish viscous solution upon dissolution of PU confirms the solubilization (Scheme 1). Viscosity measurements also show an increase in the coefficient of viscosity (η) with an increase in the amount of PU added to the DES (Fig. S7, SI). The value of η for pure LA : $ZnCl_2$ (1 : 1) DES is ~24.8 Pa s, which increases to 93.2 Pa s after the addition of 17% (w/w) of PU. It further increased to 321.2 Pa s at 34% and 561.4 Pa s at 52% PU loading to the DES, confirming efficient dissolution of PU in LA : $ZnCl_2$ (1 : 1). The dissolved PU has been regenerated by using water as an antisolvent, followed by its separation from aqueous DES *via* centrifugation (Scheme 1). The colour of the regenerated material is carbon black, in contrast to the whitish appearance of PU used in this study, which is suggestive of the depolymerization and degradation of PU during dissolution. Fig. 1 shows the comparative Fourier transform-infrared (FTIR) and X-ray photoelectron (XPS) spectra of native PU and the regenerated material. The band at ~3303 cm^{-1} corresponding

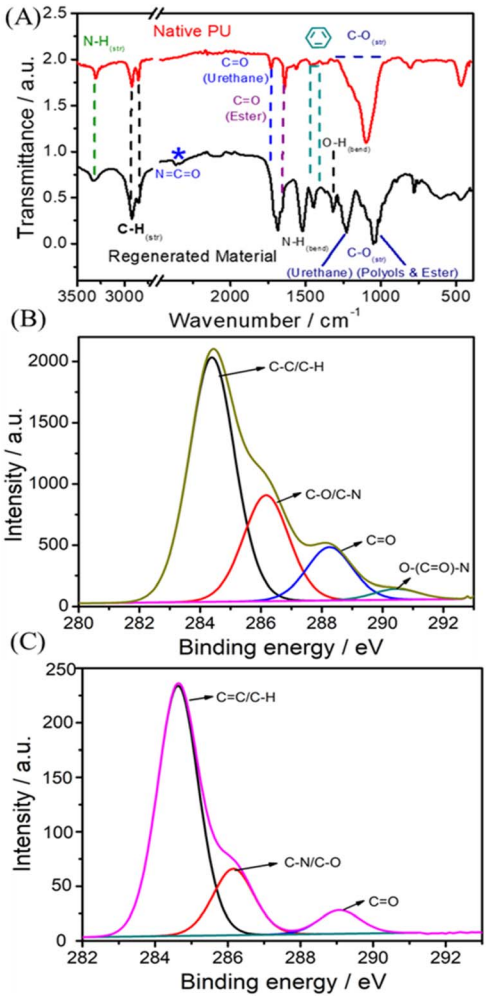

Fig. 1 (A) FTIR and (B and C) C 1s XPS spectra of the material regenerated from DES (1 : 1) in comparison to native PU.

to N–$H_{(\upsilon,s)}$ vibrations of urethane bonds in PU broadens and shifts towards blue at ~3339 cm^{-1} in the regenerated material (Fig. 1A), suggesting the prevalence of H-bonding interactions between fragmented PU units.[43,44] The formation of 2°-amines exhibiting N–$H_{(\upsilon,s)}$ cannot be ruled out at this stage. The relative change in the intensity of the bands at ~2915 cm^{-1} for C–$H_{(\upsilon,as)}$ and ~2853 cm^{-1} for C–$H_{(\upsilon,s)}$ in the native PU[13,45] along with an increase in the intensity of the bands at ~1445 cm^{-1} and ~782 cm^{-1} related to in-ring C–$H_{(\upsilon)}$ and C–$H_{(\delta)}$ vibrations of substituted benzene rings, respectively, signifies the unwinding and fragmentation of PU upon dissolution.[15,42] Two well-defined bands at ~1730 cm^{-1} and ~1640 cm^{-1} corresponding to C=$O_{(\upsilon,s)}$ of the urethane linkage and ester group, respectively, merge at 1684 cm^{-1} with shoulders at ~1714 cm^{-1} and ~1654 cm^{-1}. A broad intense C–$O_{(\upsilon)}$ band splits into two sharp bands corresponding to the C–$O_{(\upsilon)}$ of the urethane linkage (~1230 cm^{-1}) and glycols/esters in polyurethane (~1050 cm^{-1}). The merging of the C=$O_{(\upsilon)}$ band and the simultaneous splitting of a broad intense C–$O_{(\upsilon)}$ band is ascribed to structural alterations near the urethane bond related to partial or full deterioration of the urethane linkage.[46–48] The appearance of a sharp band at ~1520 cm^{-1} in the regenerated material is ascribed to the N–$H_{(\delta)}$ of the amide-II band resulting from the destruction of the urethane linkage. The breakage or structural alterations near the urethane linkage could result in the fragmentation of PU to smaller subunits with different functional groups, such as –OH and dicyanamide, which is supported by the appearance of –$OH_{(\delta)}$ at ~1320 cm^{-1} and N=C=$O_{(\upsilon)}$ at ~2320 cm^{-1} in the regenerated material.

The C 1s XPS spectra of both the native PU (Fig. 1B) and the regenerated material (Fig. 1C) display primary peaks at 284.4 eV and 284.64 eV, corresponding to C–C and C=C bonds, respectively.[47] Additional peaks are observed at ~286.16 eV and ~289.1 eV, corresponding to C–O and C=O bonds, respectively.

Notably, a distinct peak at ~290.53 eV attributed to the O–(C=O)–N functionality of the urethane bond in PU[48] disappears in the XPS spectrum for the regenerated material, signifying the cleavage of the urethane bond. Some of the urethane bonds remain as relatively higher molecular weight fragments of PU, as observed from MALDI-TOF measurements (discussed later), which are stabilized by the urethane linkage.

^{1}H and ^{13}C nuclear magnetic resonance (NMR) measurements corroborate the results obtained from FTIR and XPS measurements well (Fig. 2). Resonance peaks were systematically assigned as A onwards, starting from the most shielded proton or carbon. A substantial number of peaks (0.81–1.82 ppm) (peak A) in the ^{1}H NMR spectrum (Fig. 2A) confirm the presence of methyl (–CH_3), methylene (–CH_2), and methine (–CH) groups supported by peak A (9.54 ppm) in the ^{13}C NMR spectra of the regenerated material within the saturated hydrocarbon framework.[15] The appearance of such a large number of NMR peaks in both the ^{1}H and ^{13}C NMR spectra for

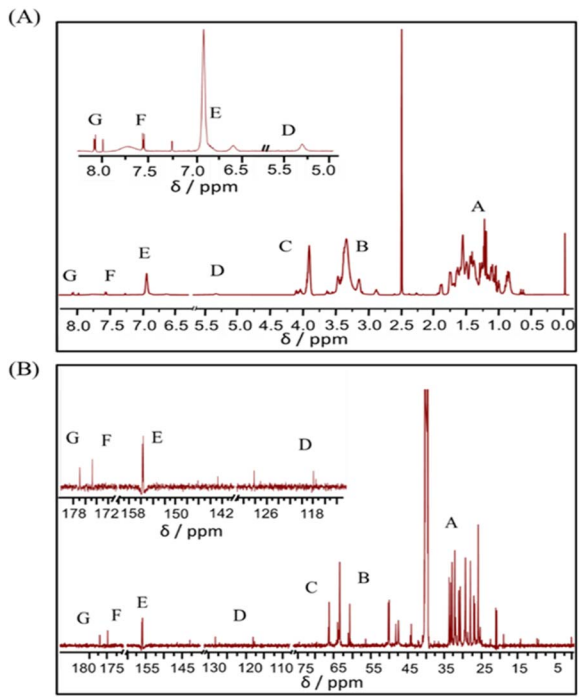

Fig. 2 (A) ^{1}H NMR; and (B) ^{13}C NMR spectra of the material regenerated from DES (1 : 1).

the regenerated material, as compared to native PU,[49,50] suggests the depolymerization of PU. The presence of amine groups in the regenerated material is established by the emergence of a resonance peak in the range 3.00–3.50 ppm (peak B) in the ^{1}H NMR spectrum, in line with observations made from FTIR spectroscopy. Different ^{1}H NMR peaks (Fig. 2A), *i.e.*, peak E (6.89 ppm); peak F (7.25 ppm); and peak G (8.07 ppm),[15,51] and ^{13}C NMR peaks (Fig. 2B), *i.e.*, peak E (143.13, 156.0 and 156.16 ppm) confirm the presence of aromatic ring protons and substituted benzene ring carbon atoms, respectively.

Similarly, the peaks at 118.25 ppm (peak D) and 128.49 ppm (peak E) support the presence of C=C of alkenes. A multiplet at ~3.30 ppm and 3.91 ppm (peak C) (Fig. 2A) indicates the presence of protons associated with the –CH_2–O (alkoxy moiety) of an ester group, which is further corroborated by multiple peaks in the range of 60.63–66.76 ppm (peak C) in the ^{13}C NMR spectrum (Fig. 2B). Two distinct peaks for C=O at 175.12 ppm (peak F) and 177.28 ppm (peak G)[36] in the ^{13}C NMR spectra establish two types of C=O groups related to broken urethane and ester bonds.[49] The absence of peaks at 153.64 ppm and 152.60 ppm (Fig. 2B), corresponding to the C=O of the urethane bond,[50] establishes the cleavage of the urethane bond. Additionally, a broad peak at 5.30 ppm (peak D) in the ^{1}H NMR spectrum and peaks at 50.14–64.76 ppm (peak B) in the ^{13}C NMR spectrum corresponding to a carbon atom attached to –CH_2OH signify the presence of hydroxyl (–OH) groups, which are otherwise absent in native PU. From the aforementioned investigations, it is inferred that the PU undergoes unwinding and degrades to smaller fragments bearing different functional groups, with some fragments retaining native molecular bonding.

The degradation of PU and the appearance of new functional products are also supported by thermogravimetric analysis (TGA) (Fig. 3A and B). Native PU undergoes a two-step thermal degradation[18,45] with a weight loss of 41.1% in the range of 280–300 °C and exhibiting onset of degradation (T_d) at ~287.50 °C owing to the decomposition of the urethane bond.[45,53] This is followed by a weight loss of ~58.6% in the temperature range of 300–455 °C ascribed to the decomposition of polymeric fragments of glycols and polyesters.[2] In contrast, the regenerated material exhibits a four-step weight loss with relatively lower T_d of ~177.8 °C, signifying the decomposition of PU. The weight loss of ~27.0% between 220 and 340 °C is associated with the decomposition of glycols. The third and fourth decomposition between ~415 and 470 °C (weight loss 33.4%) and 570–630 °C (weight loss ~17.5%) accounts for the degradation of small chain polyesters[44] and de-crosslinking of the rest of the PU, respectively.[17] Beyond 650 °C, the weight loss in the regenerated material is negligible, indicating the absence of other functional groups in the regenerated material.[21]

A decrease in intensity of the prominent X-ray diffraction (XRD) scattering peak around 2θ ~18° (Fig. S1, SI) along with a shift towards lower 2θ values in the regenerated material suggests it to be relatively disordered.[51–54] Further, the native PU exhibits a peak at 2θ ~11°, the absence of which in the regenerated material supports the cleavage of bonds of hard segments during dissolution.[45,55]

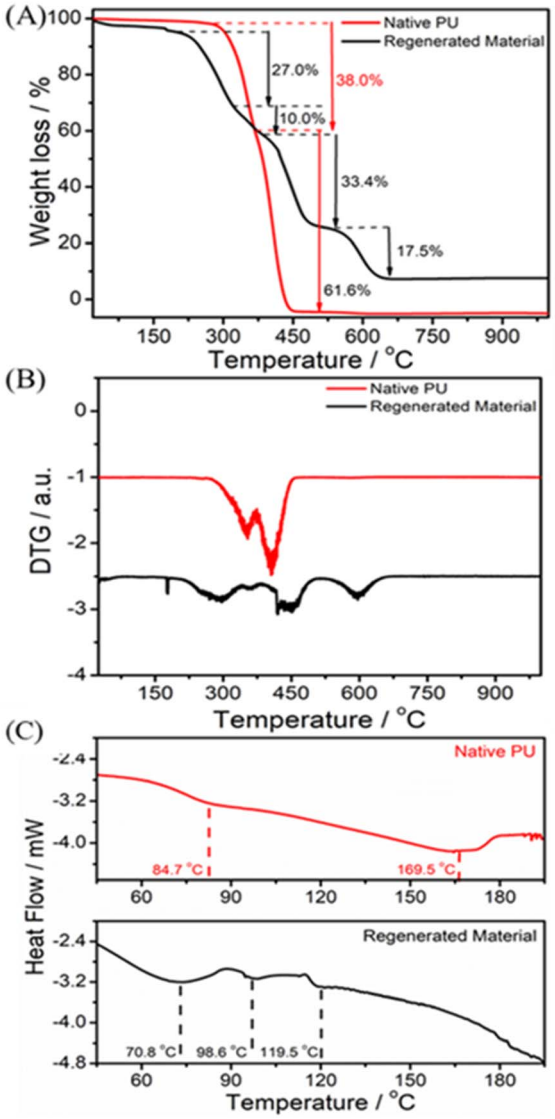

Fig. 3 (A) TGA profile, (B) DTG profile (it is scaled to show the difference) and (C) DSC thermograms of material regenerated from DES (1 : 1) in comparison to native PU.

Two weak endotherms in differential scanning calorimetry (DSC) thermograms (Fig. 3C) of PU at ~84.7 °C and ~169.5 °C[55,56] are assigned to the breakdown of soft segments and the dissociation of the crystalline hard segment having inter-urethane *H*-bonds, respectively.[49,56,57] By comparison, three endotherms at relatively lower temperatures, *i.e.*, 70.8 °C, 98.6 °C, and 119.5 °C, are observed in the regenerated material (Fig. 3C). The endotherms at ~70.8 °C and ~98.6 °C correspond to the melting of polyester/glycols of fragmented PU, while the endotherm ~119.5 °C corresponds to phase transitions in the fragments formed from the breakdown of hard segments of PU.[58–60] The appearance of endotherms at relatively lower temperatures supports the unwinding of PU, accompanied by the formation of relatively small, fragmented units with different functionalities, which can react with each other after degradation.[47,61]

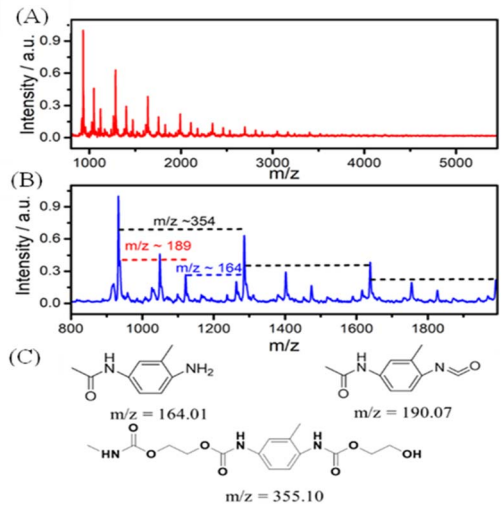

Fig. 4 (A) Mass spectrum of material regenerated from LA : $ZnCl_2$ DESs 1 : 1; (B) enlarged counterpart of (A) and (C) molecular structures of probable fragments.

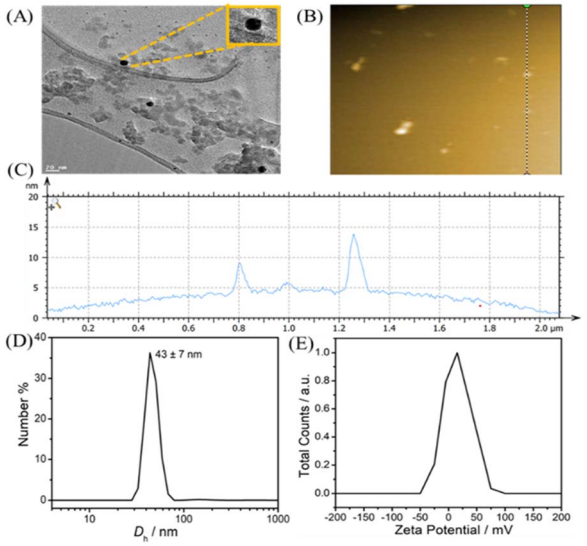

Fig. 5 (A) TEM image, (B) AFM image (C) corresponding height profiles of AFM images, (D) distribution of D_h and (E) ζ-potential of the regenerated material.

MALDI-TOF measurements provided further insights into the molecular fragments of the regenerated material (Fig. 4). The regenerated material exhibits a high-intensity peak at *m*/*z* ~934 followed by several correlated peaks at different *m*/*z* values separated by *m*/*z* ~354, where the intensity of peaks decreases while going towards higher *m*/*z* values (Fig. 4). Along with those, other fragments at *m*/*z* ~1049 and *m*/*z* ~1121 show different associated peaks separated by *m*/*z* ~354. It is natural to assume that these fragments originate from a common precursor *via* non-specific breakage of the polymeric chain, and thus are structurally correlated to each other. The analysis of the data revealed that the major fragments that correlate with three main peaks (Fig. 4) have *m*/*z* ~354, 189 and 164. It would be problematic to discuss further in this regard; however, considering the structure of PU employed and the inferences obtained from various techniques, some of the probable fragments (Fig. 4C) are proposed. Further, the non-breakage of phenyl groups and their repetitive arrangements in the regenerated material hinders it from being water soluble. The regenerated material does, however, solubilize in ethanol, DMSO, and DMA. Such solubilization indicates the induction of polar functional groups in the fragmented lower-molecular-weight PU.

These inferences are further supported by the GPC analysis of the regenerated material. A significant reduction is observed in the number average molecular weights (M_n) and weight average molecular weights (M_w) of the materials, regenerated from degraded PU in both the DESs, as compared to the molecular weight of PU (~10 000 g mol^{-1}). It is observed that the regenerated material obtained from DES (LA : $ZnCl_2$ = 1 : 1) shows the presence of at least four degraded fragments of PU correlated with peaks (M_w) at 1964, 2447, 3454, and 4631 g mol^{-1}, with relative peak areas of 12%, 35%, 22% and 31%, respectively (Fig. S8, SI). The average M_n is ~2477 and the average M_w is ~3070 g mol^{-1}. Similarly, four peaks are observed in the case of LA : $ZnCl_2$ (4 : 1) DES, with M_w ~1866, 2539, 3505, and 4464 g mol^{-1} and relative peak areas of 12%, 8%, 22%, and 58%, respectively (Fig. S8, SI). The average M_n in this case is ~2870 and the average M_w is ~3795 g mol^{-1}. These inferences support the successful degradation of PU into fragments of low molecular weights, which are ~20–30% of the molecular weight of the native form of PU.

The TEM images (Fig. 5A) indicate that the regenerated material consists of small spherical (~3–10 nm in size) as well as agglomerated particles (~80–120 nm). Small particles (Fig. 5A and B) of varying size and shape suggest the non-selective degradation of the polymer into fragments.[62] The AFM height profile shows that the particles have a thickness of ~5–10 nm and a breadth of ~50–200 nm (Fig. 5C). Dynamic light scattering (DLS) measurements (Fig. 5D) further confirm that the hydrodynamic diameter (D_h) of the particles comprising the regenerated material is in the range of 30–70 nm, corresponding to agglomerated particles. A small positive ζ-pot value ~15.4 mV (Fig. 5E) indicates the presence of functional groups that undergo dissociation or protonation in water, resulting in positively charged groups in the regenerated material.

Effect of composition of DESs

DES with a 4 : 1 molar ratio of LA and $ZnCl_2$ also dissolves PU under the given conditions. However, the extent of solubilization decreases (30 w/w%). The appearance of a less viscous solution with a brownish hue (Fig. 6A) as compared to the highly viscous black solution observed in the case of LA : $ZnCl_2$ (1 : 1) supports the decreased solubility of PU. Further, the chemical as well as elemental composition of the material regenerated from the 4 : 1 DES was found to be similar to that of the material regenerated from the 1 : 1 DES (Fig. S2, SI and 6B).

However, the material regenerated from the DES with higher LA content exhibits a relatively lesser decrease in crystalline order (Fig. S3, SI) while displaying a marginally higher thermal

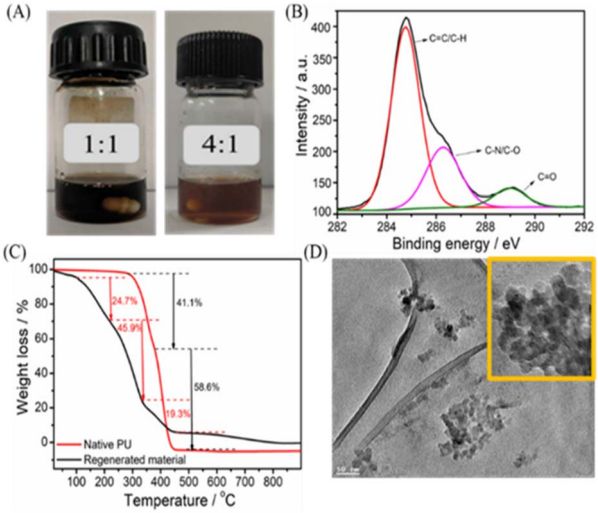

Fig. 6 (A) Images of solution of PU in DESs. (B) XPS spectra (C) TGA profile and (D) TEM image of material regenerated from 4 : 1 DES.

stability (Fig. 6C). The surface morphology of the regenerated material is also observed to be similar to that of the material regenerated from the 1 : 1 DES in addition to the formation of sheet-like structures (Fig. 6D). The regenerated material obtained from both the DESs shows similar structural features. However, the DES with a 4 : 1 LA : $ZnCl_2$ ratio is relatively less efficient in disrupting the polymeric structure, as also evident from the large number of peaks with high intensity at higher *m*/*z* values than that observed in the case of 1 : 1 LA : $ZnCl_2$ (Fig. S4, SI). This is also confirmed by the relatively lower solubility of the material regenerated from the DES with 4 : 1 LA : $ZnCl_2$ in ethanol.

Mechanism of dissolution and depolymerization

The capability of Cl^- to undergo H-bonding with the polymeric network, as observed during the dissolution of cellulose,[32] is expected to aid in the unwinding of the polymeric chains during dissolution. This is followed by $ZnCl_2$-mediated fragmentation of PU. $ZnCl_2$ is a Lewis acid, which interacts with and activates the C=O group of LA, and, in the presence of white light, the energy of the activated π-bond decreases.[23,62] As a result, a free radical is formed on the C=O group of LA, which initiates the reaction by abstraction of a proton (Scheme 2).

The free radical is regenerated on the PU chain without any selectivity, and, consequently, it extracts the proton from its immediate vicinity. The formation of free radicals during the dissolution process is confirmed by the addition of benzoquinone, a free-radical quencher, which inhibits the reaction when added to the DES. This results in the breakage of the PU chain and, following the Norrish type II mechanism, leads to the formation of an alkene chain or shorter hydrocarbon chain with different functional groups in the presence of O_2. O_2 may also combine with the free radicals formed upon abstraction of protons, resulting in oxidation of the material. It is quite likely that the C=O group of the urethane bond is also be activated by $ZnCl_2$, which, together with the activation of the C=O group of LA, results in depolymerization of PU and enhances its solubilization.

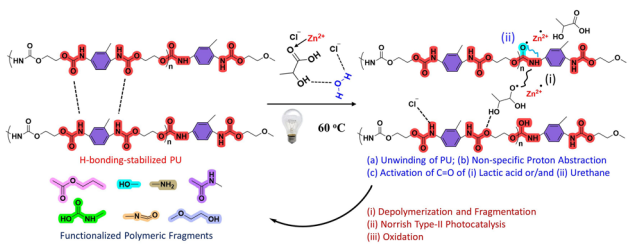

Scheme 2 Schematic presentation of the degradation of PU in DES under white light.

At 60 °C, the dissolved PU and fragmented products are anticipated to be stabilized by DES through H-bonding. This stabilization slightly reduces H-bonding interactions among the DES components, which in turn enhances the extent of PU dissolution. The free radical generated on the oxygen of LA or the urethane bond regains its structure, and DESs could be reused for the dissolution of PU. It is natural to assume that the Cl^- and OH^- could potentially cleave the bonds of PU *via* nucleophilic attack.

The varying extents of solubilization of PU in DESs with different compositions can be explained by the proposed free-radical-induced solubilization. The interaction of Zn^{2+} with C=O is expected to be more probable through a coordination bond in DES with a 1 : 1 molar ratio of LA : $ZnCl_2$. This hypothesis is supported by negligible dissolution of PU in the 1 : 1 DES in dark conditions, further pointing to the role of light in PU depolymerization.

Conversely, LA : $ZnCl_2$ (4 : 1), having a relatively higher content of LA, fosters an increased extent of intra-molecular H-bonding interactions (LA–LA) (Fig. S5, SI).[23] This, in turn, leads to a reduction in the intermolecular interactions between LA and $ZnCl_2$, thus partially hindering the activation of C=O by $ZnCl_2$. The possible coordination of the Zn^{2+} with any of the –OH groups of LA instead of the C=O group could hinder the activation of the C=O group. Therefore, in the presence of more LA, the formation of a free radical from the C=O group by Zn^{2+} through the coordination bond, required to initiate the dissolution and breakdown of PU, is less probable.

The role of individual components in the dissolution of PU under similar reaction conditions has been investigated. It is observed that individual concentrated aqueous solutions of $ZnCl_2$ [1.8 M] and LA [2.7 M] are not able to solubilize and degrade PU even after 72 h of visible light exposure (Fig. S9, SI). This observation points to the combined role of the intermolecular H-bonding network and the varied electronic structure of $ZnCl_2$ and LA in the vicinity of each other, which facilitates PU depolymerization. As discussed above, $ZnCl_2$ helps activate the C=O bond of LA and promotes proton abstraction, aiding depolymerization. This process is unlikely in the absence of either component.

Further, the recyclability of DESs has also been investigated. The DES was successfully recovered after the dissolution of PU by the separation of the dissolved material, followed by the evaporation of water. The DESs were recycled for at least three

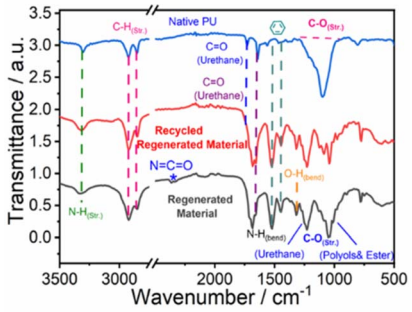

Fig. 7 FTIR spectra of native PU, regenerated material, and material regenerated from reused DES.

cycles of PU dissolution and regeneration without observing any compositional alterations in DESs. The regenerated materials from recycled DESs showed similar structural features to those regenerated from pristine DESs (Fig. 7 and S6, SI). It is inferred that PU undergoes unwinding and depolymerization *via* the breakage of the urethane bond, specifically along with other bonds, where the regenerated material has different functional groups. The present work, along with the previous reports on the processing of PU, is expected to offer a new perspective not only for solubilizing a variety of hard-to-dissolve materials in industrially relevant quantities in a sustainable way but also for functionalization or processing of such polymers for diverse applications while adhering to sustainable development goals.

Toxicity test on *Escherichia coli*

The toxicity of the regenerated material obtained by the depolymerization of PU in DES has been investigated. Growth inhibition of bacterial strains of *Escherichia coli* (*E. coli*) was taken as a model experiment to check the toxic nature of the obtained material. The results show the nonhazardous nature of the material as no inhibition zone was observed in *E. coli* cultures in the presence of both materials obtained by dissolution of PU in DES (Fig. S10, SI).

Cost-benefit analysis

The total cost incurred for the dissolution and regeneration of depolymerized PU (70 w/v%) in 1 mL of DES amounts to INR 22 899.49, which includes both capital expenditure (CapEx) and operational expenditure (OpEx) (Fig. S11, SI). A significant portion of this cost, ~96.24%, is attributed to CapEx, while OpEx constitutes only 3.76% of the total expenditure, which suggests that the initial investment in equipment and infrastructure is the primary financial burden, whereas the recurring operational costs are relatively lower. This makes the first cycle of dissolution, depolymerization and regeneration of PU in DES economically non-feasible (Annexure S3, SI), considering the processing fee of INR 50 per gram of PU. However, by considering the recyclability of DES and assuming 1000 cycles per year, the total benefits for the first year are estimated at INR 35 00 000, while the total cost for the first year stands at INR 2 22 608.93. This results in a positive net present value (NPV) of INR 29 59 209.25 for the first year, indicating a strong financial gain over time. Additionally, the benefit-cost ratio for the first operation is 15.723, meaning that for every rupee invested, ~INR 15.72 is recovered, which represents a substantial economic advantage (Annexure S3, SI). Thus, the inclusion of solvent recyclability significantly improves the financial feasibility of the process. Compared to scenarios where the solvent is not reused, the cost per cycle is greatly reduced, leading to a highly favourable NPV and benefit-cost ratio. This analysis suggests that the dissolution of PU using DES under white light can be an economically viable process when solvent reuse is implemented, making it attractive for industrial applications.

Experimental

Materials

Metal-based DESs comprising $ZnCl_2$ as the H-bond acceptor (HBA) and lactic acid (LA) as the H-bond donor (HBD) (LA : ZnCl2) in molar ratios of 1 : 1 and 4 : 1 were taken from the lot reported previously.[23] Karl–Fischer titration analysis using an automated Metrohm 831 KF Coulometer demonstrates that the used DESs are hygroscopic in nature and saturate at $ZnCl_2 : H_2O = 1 : 1$ in both DESs. Polyurethane (PU), selectophore and dimethyl sulfoxide-d_6 (DMSO-d_6) (>99.9%) were purchased from Sigma Aldrich. An analytical weighing balance (Precisia) with a precision of 0.0001 g was used to weigh the chemicals, and the dissolved PU was regenerated using degassed Millipore-grade water.

Dissolution and regeneration of polyurethane in DESs

A given amount of PU was placed in a glass vial containing 4 g of the respective DES pre-heated at 60 °C in the presence of white light (40 W LED) at atmospheric pressure and stirred at 200 rpm after obtaining an approximate idea about the extent of dissolution by adding PU in a stepwise manner (200 mg per lot). The onset of dissolution was marked by the appearance of a yellowish colour, which eventually turned blackish and more viscous with the gradual dissolution of PU. The dissolution was monitored *via* optical microscopy, where the appearance of solid particles, even after prolonged stirring (24 h), marked the saturation of dissolution. The viscosity of the DES with dissolved PU was measured using an Anton Paar MCR-92 159 000 Model modular compact rheometer using cone plate geometry (CP 25 mm). The dissolved PU was regenerated using water as the antisolvent, and the precipitated product was subsequently separated using centrifugation at 6000 rpm for 15 min. Following the separation of the regenerated material, the aqueous layer containing the respective DES was vacuum-dried, and the DES was recovered.

Characterization of regenerated material

Fourier transform-infrared spectroscopy (FTIR) measurements were performed using an Agilent Cary 630 FTIR instrument in the range of 500–4000 cm^{-1}. X-ray photoelectron spectroscopy (XPS) measurements of native PU and the regenerated material were performed on a Thermo-Scientific NEXSA spectrometer employing a monochromatic Al Kα X-ray source with magnetic focusing and a charge neutralizer operated at 1486.6 eV. Data

analysis and data processing were performed using Thermo Avantage v5.9925 software and Thermo Avantage v5.9921 software, respectively. ^{1}H and ^{13}C nuclear magnetic resonance (NMR) measurements of the regenerated material in DMSO-d_6 were performed on a JEOL, ECZR 600 MHz NMR spectrometer. Powder X-ray diffraction (XRD) measurements were performed on a Shimadzu Maxima 70 000 instrument in the 2θ range of 5–80°. Thermogravimetric analysis (TGA) was done on a Hitachi STA7200 thermal analysis system under an N_2 atmosphere in the temperature range of 25 to 1000 °C at a heating rate of 10 °C min^{-1}. A Mettler Toledo differential scanning calorimeter, DSC 3, which has a strong and adaptable DSC sensor with 56 thermocouples, was used to perform differential scanning calorimetry (DSC) at a rate of 2 °C min^{-1} under a N_2 atmosphere. Atomic force microscopy (AFM) was performed on an Anton Parr Tosca Series 400 AFM in tapping mode. Transmission electron microscopy (TEM) was performed on a JEOL JEM-2100 electron microscope, operating at 200 kV. The ethanolic solution of the regenerated material was drop-casted on mica sheets for AFM measurements and a 300 mesh carbon-coated TEM grid for TEM imaging, followed by drying at room temperature. Zeta-potential (ζ-Pot) and hydrodynamic radius (D_h) measurements were performed using a Malvern Nano-Series ZS light scattering instrument at 173° scattering angle employing a dip cell (ZEN-212) and quartz cuvette, respectively. MALDI-TOF-MS measurements and analyses were carried out using a Bruker Autoflex III. Size-exclusion chromatography (SEC) was performed on a 1260 Infinity II GPC MDS System connected to GPC-specific detectors, namely a RID, a viscometer, and a dual-angle LSD system. The system was equipped with a 1260 Infinity II isocratic pump, two guard columns (PLgel 5 μm Guard 50 × 7.5 mm), a 1260 Infinity II vial sampler, a 1260 Infinity II multicolumn thermostat (MCT) at 50 °C, with two PLgel (5 μm, MIXED-D 300 × 7.5 mm) columns in series. A 1260 Infinity II Diode Array Detector (DAD), a refractive index detector (RID), and a viscometry detector were used to analyze the samples. DMAc containing 5 g L^{-1} of LiCl was used as the eluent at a flow rate of 0.5 mL min^{-1}. The spectra were analyzed using the Agilent GPC/SEC software dedicated to multi-detector GPC calculations. The molar mass and dispersity values were calculated against PMMA standard.

Toxicity test on *E. coli*

E. coli strain (ATCC 25922) was inoculated for 24 h on nutrient broth at 37 °C. It was subjected to the Kirby Bauer disc diffusion toxicity test to determine the nonhazardous nature of the regenerated material from both DESs. A loop full of bacteria was spread on a nutrient agar plate and 50 μL of materials A and B was loaded and incubated at 37 °C for 48 h.

Conclusion

Polyurethane (PU) has extensive commercial use, but its non-biodegradability and lower solubility in conventional solvents under sustainable conditions hamper its recyclability and pose serious environmental problems like bioaccumulation. Along these lines, we developed an efficient and sustainable method for the dissolution and depolymerization of PU in neat LA : $ZnCl_2$ DESs (1 : 1) under white light at an ambient temperature of 60 °C. The impact of varying the molar ratio of the DESs on the dissolution of PU was investigated. DES composing LA : $ZnCl_2$ in a 1 : 1 molar ratio shows the maximum efficiency for PU dissolution of 70 w/w% whereas the dissolution power of DES decreases to 30 w/w% with the increase in the LA content in DES from a molar ratio of 1 : 1 to 4 : 1. Herein, we have shown for the first time that neat DESs, without the addition of any solvent, can degrade PU into small fragments bearing different functional groups in the presence of air at low temperature under normal pressure conditions in a short time. The reusability of DESs contributes to the process's sustainability, where it is used again for dissolving PU. It is also important to mention the fact that the components of DESs are benign, biodegradable, and cost-effective, which could open up new commercial opportunities and eventually aid in the dissolution and degradation of other synthetic polymers.

Author contributions

Harmandeep Kaur (major experimentation, data analysis and drafting of manuscript); Rajwinder Kaur (experimentation and data analysis); Muskan (data analysis and discussions); Manpreet Singh (data analysis and discussions); Ravi Dutt (data analysis and discussions); Kanica Sharma (data analysis and discussions); Harjinder Singh (data analysis); Kuldeep Singh (experimentation and discussions); Arvind Kumar (conceptualization and data analysis); Gurbir Singh (data analysis, discussions, review and writing manuscript) Tejwant Singh Kang (funding, conceptualization, supervision, data analysis and manuscript writing). All authors have given approval to the final version of the manuscript.

Conflicts of interest

There are no conflicts to declare.

Data availability

The data will be made available on request.

Supplementary information (SI) is available. See DOI: https://doi.org/10.1039/d5su00436e.

Acknowledgements

We are grateful to UGC, India, for their UGC-CAS program and DST, India, for the FIST program awarded to the Department of Chemistry, Guru Nanak Dev University, Amritsar. H. K. (SRF), R. K., (SRF), M. S., (SRF), M. (JRF), R. D. (NFSC), K. S. (SPM-SRF) and H. S. (SRF) are thankful to UGC and CSIR, Govt. of India, for fellowship. We are highly thankful to Dr Karthikeyan Sekar (Assistant Professor) and his team, Department of Chemistry, SRM Institute of Science and Technology, Kattankulathur, Tamil Nadu, India, for their contribution to the GPC analysis for this work.

References

1 N. Saikia and J. De Brito, *Constr. Build. Mater.*, 2012, **34**, 385–401.
2 G. Trovati, E. A. Sanches, S. C. Neto, Y. P. Mascarenhas and G. O. Chierice, *J. Appl. Polym. Sci.*, 2010, **115**, 263–268.
3 D. K. Chattopadhyay and K. V. S. N. Raju, *Polym. Sci.*, 2007, **32**, 352–418.
4 K. M. Zia, H. N. Bhatti and I. A. Bhatti, *React. Funct. Polym.*, 2007, **67**, 675–692.
5 G. T. Howard, *Biodegradation*, 2002, **49**, 245–252.
6 W. Yang, Q. Dong, S. Liu, H. Xie, L. Liu and J. Li, *Procedia Environ. Sci.*, 2012, **16**, 167–175.
7 S. J. McCarthy, G. F. Meijs, N. Mitchell, P. A. Gunatillake and G. Heath, *Biomater.*, 1997, **18**, 1387–1409.
8 J. O. Akindoyo, M. Beg, S. Ghazali, M. R. Islam, N. Jeyaratnam and A. R. Yuvaraj, *RSC Adv.*, 2016, **6**, 114453–114482.
9 J. Schmidt, R. Wei, T. Oeser, L. A. Dedavid e Silva, D. Breite and A. Schulze, *Polymers*, 2017, **9**, 65.
10 R. S. Labow, E. Meek and J. P. Santerre, *Biomater*, 2001, **22**, 3025–3033.
11 A. S. Mathew, K. Sreenivasan, P. V. Mohanan, T. V. Kumary and M. Mohanty, *Trends Biomater. Artif. Organs*, 2006, **19**, 115–121.
12 D. K. Chattopadhyay and D. C. Webster, *Prog. Polym. Sci.*, 2009, **34**, 1068–1133.
13 L. Q. Wang, G. Z. Liang, G. C. Dang, F. Wang, X. P. Fan and W. B. Fu, *Chin. J. Chem.*, 2005, **23**, 1257–1263.
14 S. Thomas, A. V. Rane, K. Kanny, V. K. Abitha and M. G. Thomas, *Recycling of Polyurethane Foams, William Andrew, an Imprint of Elsevier*, Oxford; Cambridge, MA, 2018.
15 Y. Wang, H. Song, H. Ge, J. Wang, Y. Wang, S. Jia and X. Hou, *J. Clean. Prod.*, 2018, **176**, 873–879.
16 S. Mondal and D. Martin, *Polym. Degrad. Stab.*, 2012, **97**, 1553–1561.
17 S. Pashaei, H. Siddaramaiah and A. A. Syed, *J. Macromol. Sci., Part A: Pure Appl. Chem.*, 2010, **47**, 777–783.
18 L. Jiao, H. Xiao, Q. Wang and J. Sun, *Polym. Degrad. Stab.*, 2013, **98**, 2687–2696.
19 L. D. Ellis, N. A. Rorrer, K. P. Sullivan, M. Otto, J. E. McGeehan, Y. Román-Leshkov and G. T. Beckham, *Nat. Catal.*, 2021, **4**, 539–556.
20 F. Xie, T. Zhang, P. Bryant, V. Kurusingal, J. M. Colwell and B. Laycock, *Prog. Polym. Sci.*, 2019, **90**, 211–268.
21 S. Ügdüler, K. M. Van Geem, M. Roosen, E. I. Delbeke and S. De Meester, *Waste Manag.*, 2020, **104**, 148–182.
22 H. Zhang, J. Wu, J. Zhang and J. He, *Macromolecules*, 2005, **38**, 8272–8277.
23 Y. Li, J. Wang, X. Liu and S. Zhang, *Chem. Sci.*, 2018, **9**, 4027–4043.
24 R. Ferreira, H. Garcia, A. F. Sousa, M. Petkovic, P. Lamosa, C. S. Freire, J. D. S. Armando, N. R. Paulo and C. S. Pereira, *New J. Chem.*, 2012, **36**, 2014–2024.
25 K. Aruchamy, M. Bisht, P. Venkatesu, D. Kalpana, M. R. Nidhi, N. Singh and S. K. Nataraj, *Green Chem.*, 2018, **20**, 3711–3716.
26 H. Kaur, M. Singh, K. Singh, A. Kumar and T. S. Kang, *Green Chem.*, 2023, **25**, 5172–5181.
27 A. P. Abbott, G. Capper, D. L. Davies, R. K. Rasheed and V. Tambyrajah, *Chem. Commun.*, 2003, 70–71.
28 A. Paiva, R. Craveiro, I. Aroso, M. Martins, R. L. Reis and A. R. C. Duarte, *ACS Sustain. Chem. Eng.*, 2014, **2**, 1063–1071.
29 E. L. Smith, A. P. Abbott and K. S. Ryder, *Chem. Rev.*, 2014, **114**, 11060–11082.
30 D. Xiong, Y. Wang, H. Ma, L. Lu, Q. Zhang, Y. Shi, Z. Yang and J. Wang, *ACS Sustain. Chem. Eng.*, 2022, **11**, 399–406.
31 C. Alvarez-Vasco, R. Ma, M. Quintero, M. Guo, S. Geleynse, K. K. Ramasamy and X. Zhang, *Green Chem.*, 2016, **18**, 5133–5141.
32 P. J. Piedade, V. Venkat, K. W. Al-Shwafy, M. A. Aregawi, G. Dudek, M. Zygadło and R. M. Lukasik, *New J. Chem.*, 2024, **48**, 16015–16025.
33 M. Sharma, C. Mukesh, D. Mondal and K. Prasad, *RSC Adv.*, 2013, **3**, 18149–18155.
34 D. S. Freitas, D. Rocha, T. G. Castro, J. Noro, V. I. Castro, M. A. Teixeira and C. Silva, *ACS Sustain. Chem. Eng.*, 2022, **10**, 7974–7989.
35 E. M. Nuutinen, P. Willberg-Keyriläinen, T. Virtanen, A. Mija, L. Kuutti, R. Lantto and A. S. Jääskeläinen, *RSC Adv.*, 2019, **9**, 19720–19728.
36 H. Kaur, M. Singh, H. Singh, M. Kaur, G. Singh, K. Sekar and T. S. Kang, *Green Chem.*, 2022, **24**, 2953–2961.
37 B. Liu, W. Fu, X. Lu, Q. Zhou and S. Zhang, *ACS Sustain. Chem. Eng.*, 2019, **7**, 3292–3300.
38 Q. Wang, X. Yao, Y. Geng, Q. Zhou, X. Lu and S. Zhang, *Green Chem.*, 2015, **17**, 2473–2479.
39 B. Agostinho, A. J. Silvestre and A. F. Sousa, *Green Chem.*, 2022, **24**, 3115–3119.
40 X. Song, W. Hu, W. Huang, H. Wang, S. Yan, S. Yu and F. Liu, *Chem. Eng. J.*, 2020, **388**, 124324.
41 H. Zhang, X. Cui, H. Wang, Y. Wang, Y. Zhao, H. Ma and T. Deng, *Polym. Degrad. Stabil.*, 2020, **181**, 109342.
42 A. S. Maraddi, M. H. Mruthunjayappa, S. V. Kamath, G. D'Souza, H. Yoon and S. K. Nataraj, *Green Chem.*, 2023, **25**, 10538–10548.
43 D. Rosu, L. Rosu and C. N. Cascaval, *Polym. Degrad. Stab.*, 2009, **94**, 591–596.
44 R. H. Aguirresarobe, L. Irusta and M. J. Fernandez-Berridi, *Polym. Degrad. Stab.*, 2012, **97**, 1671–1679.
45 M. Osman, S. M. Satti, A. Luqman, F. Hasan, Z. Shah and A. A. Shah, *Polym. Environ.*, 2018, **26**, 301–310.
46 A. A. Shah, F. Hasan, J. I. Akhter, A. Hameed and S. Ahmed, *Ann. Microbiol.*, 2008, **58**, 381–386.
47 X. F. Yang, C. Vang, D. E. Tallman, G. P. Bierwagen, S. G. Croll and S. Rohlik, *Polym. Degrad. Stabil.*, 2001, **74**, 341–351.
48 C. N. Young, C. R. Clayton, J. P. Yesinowski, J. H. Wynne and K. E. Watson, *Prog. Org. Coat.*, 2014, **77**, 232–241.
49 D. Allan, J. H. Daly and J. J. Liggat, *Polym. Degrad. Stab.*, 2019, **161**, 57–73.
50 D. J. Harris, R. A. Assink and M. Celina, *Macromolecules*, 2001, **34**, 6695–6700.

51 C. M. Dick, C. Denecker, J. J. Liggat, M. H. Mohammed, C. E. Snape, G. Seeley and P. Chaffanjon, *Polym. Int.*, 2000, **49**, 1177–1182.
52 G. R. da Silva, A. da Silva-Cunha Jr, F. Behar-Cohen, E. Ayres and R. L. Oréfice, *Polym. Degrad. Stab.*, 2010, **95**, 491–499.
53 T. S. Velayutham, W. H. Abd Majid, A. B. Ahmad, Y. K. Gan and S. N. Gan, *J. Appl. Polym. Sci.*, 2009, **112**, 3554–3559.
54 R. C. M. Dias, A. M. Góes, R. Serakides, E. Ayres and R. L. Oréfice, *Mater. Res.*, 2010, **13**, 211–218.
55 S. S. Umare and A. S. Chandure, *Chem. Eng. J.*, 2008, **142**, 65–77.
56 R. W. Seymour and S. L. Cooper, *Macromolecules*, 1973, **6**, 48–53.
57 D. J. Martin, G. F. Meijs, P. A. Gunatillake, S. J. McCarthy and G. M. Renwick, *J. Appl. Polym. Sci.*, 1997, **64**, 803–817.
58 J. T. Koberstein, I. Gancarz and T. C. Clarke, *J. Polym. Sci., Part B: Polym. Phys.*, 1986, **24**, 2487–2498.
59 J. G. Dillon and M. K. Hughes, *Biomater*, 1992, **13**, 240–248.
60 A. Ludwick, H. Aglan, M. O. Abdalla and M. Calhoun, *J. Appl. Polym. Sci.*, 2008, **110**, 712–718.
61 M. Špírková, M. Serkis, R. Poręba, J. Hodan, J. Kredatusová, D. Kubies and A. Zhigunov, *Polym. Degrad. Stab.*, 2016, **125**, 115–128.
62 T. T. X. Hang, N. T. Dung, T. A. Truc, N. T. Duong, B. Van Truoc, P. G. Vu and M. G. Olivier, *Prog. Org. Coat.*, 2015, **79**, 68–74.